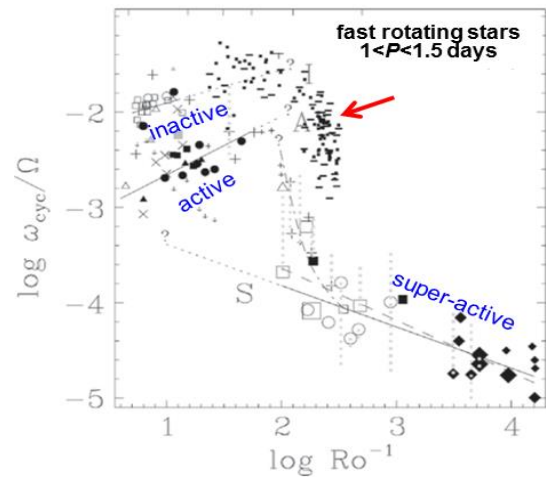
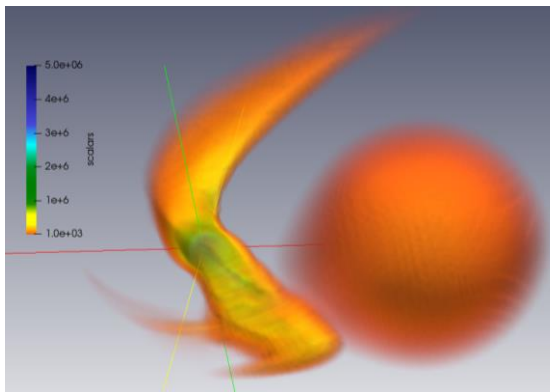


Stellar-planetary interactions and magnetospheric electrodynamics.

The problem of stellar-planetary interactions, including impact of stellar radiation and plasma flows on planetary environments and evolution of planetary systems appears among the major challenges of modern space physics. The optical and spectral phenomena, measured during exoplanetary transits, as well as in-situ data from space missions in the Solar System, provide a valuable information for probing and characterization of planetary systems and their dynamical environments. The study is focused on the topics of *stellar/solar activity*, *stellar plasmas and radiative impacts* on planetary environments. Significant accent in that respect is made on exoplanets, especially regarding the phenomena of *exoplanetary mass loss* and *magnetospheric protection*, as well as remote *observational diagnostics*. These topics are addressed in the following interrelated research directions.

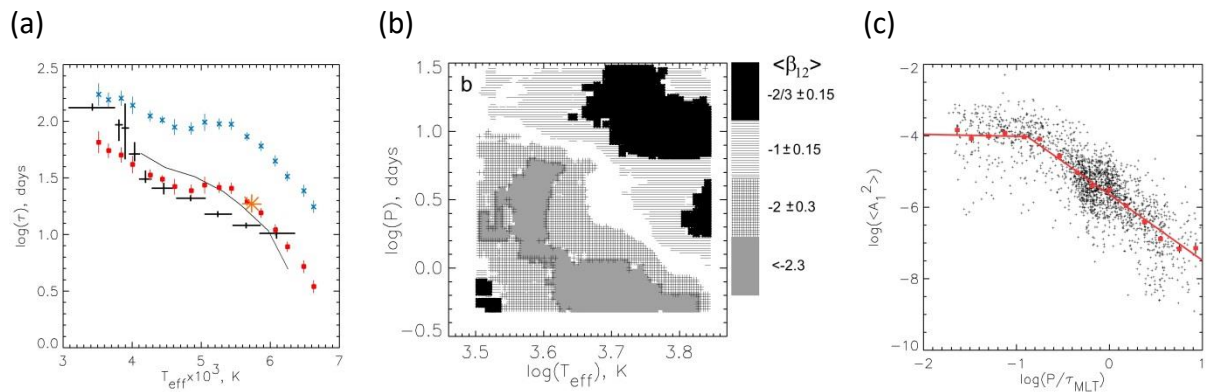
- 1) *Stellar activity and starspot diagnostics with high precision photometry* [2], [6], [7], [8], [9], [10], [11]
- 2) *The Sun as a proxy of star: Investigation of solar activity phenomena and wind patterns* [12], [13], [14], [16], [17], [18], [29], [30], [46], [47], [48]
- 3) *Global self-consistent 3D (M)HD modelling of exoplanets immersed in the stellar wind flows and remote observational diagnostics of their environments* [15], [19], [20], [21], [22], [23], [24], [25], [26], [27], [31], [38], [39], [40], [41], [42], [43], [44], [45]
- 4) *In-transit photometric sensing of exoplanetary dusty environments, exorings, exomoons* [3], [4], [5]
- 5) *Exoplanetary magnetospheres and radio emissions in MHD and plasma kinetic approaches* [1], [22], [25], [28], [32], [33], [34], [35], [36], [37], [49]



Left: The outflowing proton density distribution around hot Jupiter HD209458b, immersed in the stellar wind of its solar-type parent star, simulated with the global self-consistent gas dynamic 3D model (logarithmic scale). The planet is located at the intersection of coordinate axes. **Right:** Clustering of a set of fast rotating stars over a new specific branch (marked with red arrow) that connects the branches of inactive and super-active stars. Its formation is due to α -quenching effect, which saturates the magnetic dynamo and decreases the stellar activity cycle periods with the increase of the inverted Rossby number.

1) *Stellar activity and starspot diagnostics with high precision photometry*: Our analysis algorithms, which deal with dynamics of stellar surface activity pattern, being applied to high precision stellar light curves from the Kepler mission, enable probing of complex motions in the stellar interiors, so far inaccessible to astero-seismology methods. The measured timescales τ_1 and τ_2 of the variability of squared amplitudes of the 1st and 2nd rotational harmonics (A_1^2 , A_2^2) of stellar light-curves reveal quantitative estimates for the deep mixing turnover time τ_{MLT} – a crucial parameter in the stellar mixing length theory (MLT) – opening a way for model-independent diagnostics of the stellar deep super-large-scale convection. The analysis of gradient function $\beta_{12} = [\log(\tau_2) - \log(\tau_1)]/\log(2)$ allows differentiating of stars in the rotation period – effective temperature (P - T_{eff}) parameter space with respect to dominating mechanism of their spot variability, opening insights in physics of their dynamos. The values of $\beta_{12} = -2/3$, -2 , <-2 , and -1 correspond to the domination of Kolmogorov's turbulence, magnetic diffusion, sub-diffusion, and differential rotation, respectively. Besides of that, the known connection between sunspots and solar X-ray sources enables developing of an accessible proxy for the stellar X-ray emission on the basis of the starspot variability. The squared amplitude of 1st rotational harmonic of a stellar light curve A_1^2 is used as an activity index, related with a varying number of starspots. It reveals practically the same connection with the Rossby number as the commonly used ratio of the X-ray to bolometric luminosity, and therefore, allows elaborating of the crucial for stellar-planetary relations regressions for the stellar X-ray luminosity $L_x(P, T_{\text{eff}})$ and its related EUV analogue, L_{EUV} , for the wide range of main-sequence stars, including also those appeared below the detection threshold for the direct measurement of X-ray fluxes.

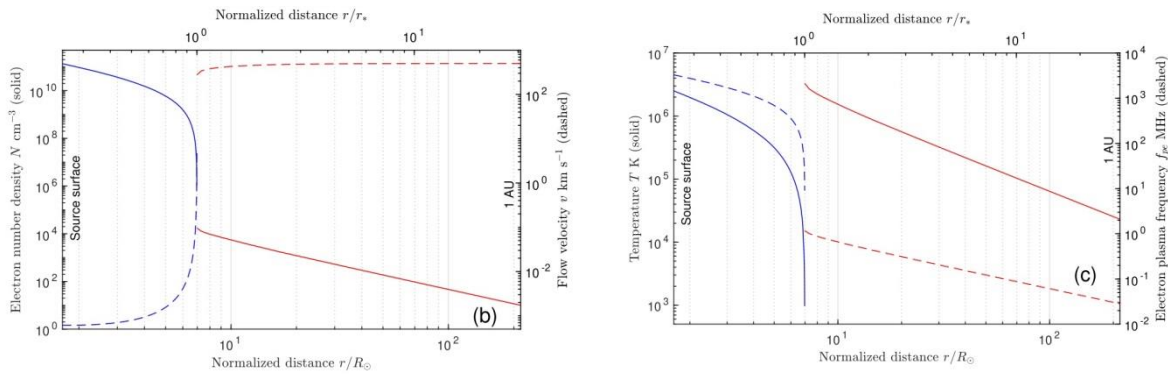
Using A_1^2 as stellar activity index, the periods of the Rieger-type cycles (RTC) were studied for 1726 main-sequence stars with different effective temperatures T_{eff} and rotation periods P observed by the Kepler space telescope. By measuring the power indexes D and D' in the functional dependencies of stellar RTC periods: $P_{\text{RTC}}(P) \sim P^D$ and $P_{\text{RTC}}(T_{\text{eff}}) \sim T_{\text{eff}}^{D'}$ two kinds of the RTCs were found: 1) activity cycles with P_{RTC} independent on the stellar rotation ($D=0$), typical for the stars with $T_{\text{eff}} < 5500$ K, and 2) activity cycles with P_{RTC} proportional ($D=1$) to P , realized on the stars with $T_{\text{eff}} > 6300$ K. These two types of RTCs can be driven by the Kelvin and Rossby waves, respectively. The Rossby wave-driven RTCs show relation with the location of tachocline at shallow depths in the hot stars, whereas the Kelvin wave-driven cycles do not show such relation.



(a) averaged timescale (blue crosses) of the 1st rotational harmonic of stellar light curves and its extrapolation to the laminar convection scale (red dots) in comparison with the standard semi-empirical estimates of the mixing length theory's turnover time τ_{MLT} according to Wright et al.(2011) - black symbols, and Landin et al. (2010) - solid line. **(b)** Diagnostic diagram of a stellar sample of 1998 main-sequence stars observed by Kepler mission with respect to a dominating mechanism of spot variability. **(c)** $\langle A_1^2 \rangle$ stellar activity index vs. the log of Rossby number.

2) *The Sun as a proxy of star – Investigation of Solar activity events and wind patterns:* The diagnostics approach for the solar coronal plasma based on the analysis of dynamic radio spectra in 8-32 MHz range is elaborated. It reveals that the physical parameters of coronal plasma before CMEs considerably differ from those during the propagation of CMEs. The local density profiles and the characteristic spatial scales of radio emission sources vary with radial distance more drastically during the CME propagation, as compared to the cases of quasistationary solar atmosphere without CME(s). This fact enables distinguishing between different regimes of plasma state in the solar corona and developing novel tools for the coronal plasma studies, using radio dynamic spectra. Besides of that, we measure the rotation rates of the solar coronal holes with the four-hour cadence data and track variable positions of their geometric centres taken from the synoptic maps of SPOCA feature monitoring system. This makes it possible to judge on the latitudinal dependence of the horizontal motions of open magnetic field structures and their transformation to the Corrotating Interaction Regions (CIRs) in the solar corona. Another important aspect of our investigations concerns the dynamic properties of coronal jets outflowing from the bright points that are embedded in coronal holes. Further, our original technique, developed for the analysis of oscillatory patterns in the flaring solar coronal loops, enables studying and interpretation of their quasi-periodic dynamical features observed as bright blobs in solar active regions. The method has potential for parametrization of the longitudinal (acoustic) wave energy sources in the flaring loops and evaluation of their role in the overall energy budget of the solar corona. In addition, based on the properties of the observed long-period (of the order of few hours) oscillations in active regions, we can deduce an appropriate depth of the related sunspot patterns, which appeared consistent with the estimations, made with the helioseismology methods. Last but not least, a new class of one-dimensional solar wind models was developed within the general polytropic, single-fluid hydrodynamic framework for the case of quasi-adiabatic radial expansion with a localized heating source. The considered analytical solutions with continuous Mach number over the entire radial domain admit the jumps in the flow velocity, density, and temperature, provided that there exists an external source of energy in the vicinity of the critical point. This is substantially distinct from the standard Parker solar wind model as well as the nozzle solutions. The discontinuous patterns of the solar wind in the inner heliosphere, predicted by our analytic model, and the complex structure of the solar wind in its source region are now observationally evidenced by the Parker Solar Probe mission.

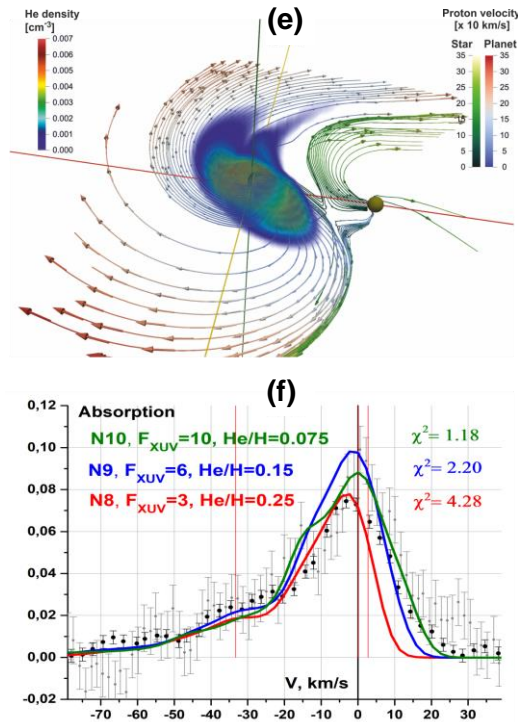
(d)



(d) The slow solar wind pattern with the sub- (blue curves) and supersonic (red curves) parts. Bottom and top abscisses stay for the distance r , scaled in units of the solar R_{Sun} and the transitionpoint r_* radii, respectively. Left panel shows the number density N (solid line, left ordinate) and flow velocity V (dashed line, right ordinate); Right panel shows the temperature T (solid line, left ordinate) and electron plasma frequency f_{pe} (dashed line, right ordinate).

3) *Global self-consistent 3D (M)HD modelling of exoplanets immersed in the stellar wind flow:*

A 3D fully self-consistent multi-fluid hydrodynamic model was elaborated for the simulation of H-He expanding upper atmospheres of hot close-orbit exoplanets (hot Jupiters and warm Neptunes), driven by the stellar XUV radiation and gravitational forces and interacting with the stellar wind. Among distinguishing features of the model are 1) 3D geometry; 2) inclusion of gravitational effects and realistic stellar radiation spectra; 3) account of the planetary dipole magnetic field; 4) self-consistent treatment of the stellar radiation and SW impacts on exoplanetary environments and the related atmospheric mass loss; 5) account of multi-fluid



(e): The modelled 3D distribution of He, in the escaping PW of WASP-107b. The PW and SW flows are shown with the colored streamlines. The planet is at the center of coordinate and moves anti-clockwise relative its star (green sphere). **(f):** He (10830Å) absorption profiles, simulated for different He abundances and stellar radiation fluxes, versus observations.

nature of the planetary and stellar material flows and the corresponding photo-chemistry. The model is free of any artificial assumptions regarding the stellar radiation flux (to significant extend measurable and constrained by the nature of star) and/or stellar and planetary material interaction scenarios, as well as the role of different physical processes to be included. The simulated with the model 3D dynamical environments of hot exoplanets enable calculation of their related transit absorption in various spectral lines, including Ly α , metastable HeI 10830 Å line, and the lines of different heavy trace elements (e.g., O, C, Si, Na, Ca, Mg, K, Fe). In the most general case, an upper atmosphere of the modelled exoplanet is taken to consist of H, H⁺, H₂, H₂⁺, H₃⁺, He, He⁺ and He₂⁺ components, for which the equations of continuity, momentum, and energy are solved numerically, and the full set of related chemical reactions is calculated. For each host star, an appropriate XUV spectrum in the range of 10-912 Å is used, including the appropriately estimated near-IR and near-UV parts. The transmission and attenuation of the stellar radiation flux is calculated in each spectral interval in accordance with the wavelength-dependent absorption cross-sections. Along with the escaping exoplanetary atmosphere, the model simulates,

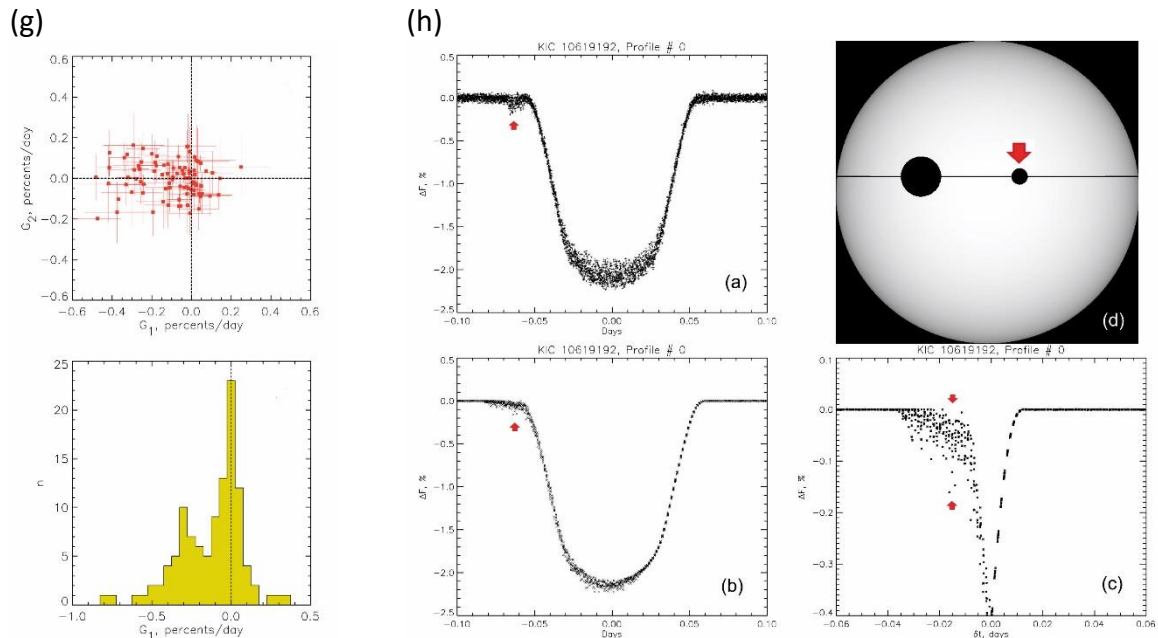
with the same numeric algorithms, the stellar wind (SW), enabling therefore a self-consistent global view of the interacting planetary and stellar material flows at the scale of the entire stellar system. The code solver is fully parallelized for performing on HPC facilities.

Magnetic field, is a crucial factor that affects the atmosphere mass loss and overall evolution of the planetary environments. Its protective role has two major aspects. First, the large-scale magnetic fields and electric currents, related with the planetary magnetism, form the planetary magnetosphere, which acts as a barrier for the upcoming stellar wind. Second, the internal magnetic field of magnetosphere influences the streaming of expanding upper atmospheric material, and therefore affects its escape and interaction with the stellar wind. Our magnetohydrodynamic modelling enables quantifying the influence of the planetary magnetic field on the upper atmospheric mass loss and planetary stransit spectroscopy

features. In particular, for the hot jupiter HD209458b, the structure and behavior of planetary magnetosphere were simulated paying attention to possible influence of the planetary magnetic field on dynamics of escaping upper atmospheric material and the measured transit absorption profiles. Fitting of the simulation results to observations enabled constraining the stellar XUV flux and helium abundance at $\sim 10 \text{ erg cm}^{-2} \text{ s}^{-1}$ at 1 a.u. and $\text{He}/\text{H} \approx 0.02$, respectively, as well as setting an upper limit for the magnetic dipole moment of HD209458b. The latter appeared to be less than 6% of the Jovian value. The self-consistent modelling of the magnetic field topology and related electric current system structure in exoplanetary magnetospheres is also crucial for the estimation of power and efficiency of the related radioemission sources and their detectability on Earth.

The global self-consistent 3D (M)HD multi-fluid model is widely used for the simulation of magnetized and non-magnetized dynamical environments of various exoplanets and interpretation of their transit spectroscopy observations and possible radio emission properties. Among the simulated planets are **HD209458b**, **HD189733b**, **WASP-107b**, **WASP-80b**, **WASP-12b**, **GJ-436b**, **GJ-3470b**, **TOI-421b,c**, and **π Men C**.

4) In-transit photometric sensing of exoplanetary dusty environments, exorings, and exomoons: The changes in duration, depth, and asymmetry of the transit light curve (TLC) profiles contain unique information about such hitherto unexplored phenomena, like exoplanetary rings, exomoons, dust tails and halos, as well as related with them dynamic phenomena in a close vicinity of exoplanets. A special role here is played by various kinds of dusty obscuring matter (DOM) structures around the planets (e.g., rings, disks, jets, and clouds), which result in additional absorption of the light and distort the regular shape of the TSCs in the region of their edges, including ingress- and egress- areas.



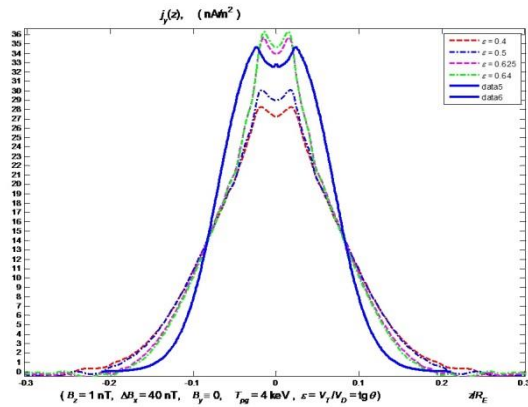
(g) Distributions of pre-transit (G_1) and post-transit (G_2) gradients of TLC estimated in the adjoining regions between 0.01 and 0.05 days, before and after the transit borders for a preselected set of 118 KOI objects. Top panel: G_2 vs. G_1 diagram; Bottom panel: histogram of G_1 estimates. **(h)** Modeling of the pre-transit DOM manifestations (arrowed) in the case of KIC 10619192. Top-left panel: real folded TLC; Top-right panel: model geometry with the real planet, crossing the stellar disk along the solid line together with a simplified sporadic DOM precursor (arrowed); Bottom-left panel: model-based synthetic folded TLC; Bottom-right panel: clipped TLC to visualize the synthetic DOM effect.

A methodology for analyzing the form of TLCs, to reveal transit anomalies and non-stationary effects associated with the presence of DOM, was elaborated. The proposed approach allows independent analysis of different parts of the TSCs and the related timing parameters such as start-/end- and minimum-time of transit, as well as the asymmetry of the TSC profile. The analysis algorithm also treats the adjacent pre- and post- transit parts of the TSC. Along with that, a special technique, to gain information about the shape of the transiting planet's silhouette, using the derivatives of TLC during the ingress and egress phases, was proposed. These methodologies are not associated with any a-priori assumptions regarding the shape of the transiting object and the presence of dust in its vicinity. They can be applied for a massive survey of a large number of objects. The discovered variability of transit timing parameters and the signs of sporadic additional absorption in the pre-transit parts of TLCs indicate on large-scale non-stationary processes in the atmospheres of some of the considered Kepler objects, as well as on dust and aerosol generation in their upper layers and in their close vicinity. The related photometry effects may be caused by dusty atmospheric outflows, erosion and/or tidal decay of moonlets, or background circumstellar dust accumulated in electrostatic or magnetic traps near the mass-losing exoplanet.

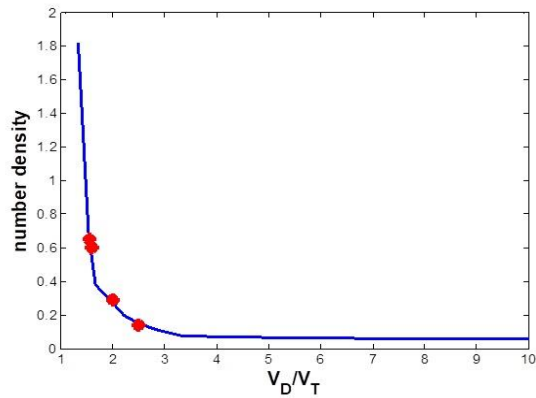
5) Exoplanetary magnetospheres and radio emissions in MHD and plasma kinetic approaches:

A key subject in this topical study concerns the self-consistent kinetic description of charged particles dynamics in astrophysical plasma-magnetic structures. The exact account of particle trajectory details and motion features (e.g., the phase of gyration) are of crucial importance for understanding of fine structure and energetics of the fundamental current-carrying systems in space plasmas, such as neutral current sheets, magnetodisks, and magnetotails.

(i)



(j)



(i) The distribution of electric current across a TCS, calculated with the analytic solutions of trajectory method (solid blue line) and simulated by numerical PIC model (dashed lines). Different colors of dashed lines correspond to different PIC modelling runs with different values of the speed of incoming particle flow ranging from $v_D/v_T=1.56$ to 2.5 . The simulations confirm theoretical prediction that v_D weakly affects the TCS scale. **(j)** The dependence of the external background proton number density on the speed of incoming particle flow (v_D/v_T), calculated with the analytic solutions of trajectory method (blue line) and simulated by numerical PIC model (red points). The simulations agree with the theoretical model prediction that in a self-consistently balanced TCS the increase of v_D/v_T leads to decrease of the background number density of protons.

We elaborate a method for the description of particle dynamics, based on a new system of differential equations for the particle pitch-angle and phase of gyro-rotation derived from the analysis of the particle trajectory in a given magnetic field. It enables a self-consistent

description of a number of basic problems, which form fundamentals for more complex natural cases of the planetary magnetospheres and in space plasmas. Further generalization of this trajectory method to a group of particles allows developing a self-consistent symmetric thin current sheet (TCS) model by adjusting of an appropriate flow of the current-producing particles and the corresponding distribution functions. This model enables, in particular, to elaborate a physically consistent theory of the TCS scalings, to study their dependence on the speed of TCS incoming plasma (V_D) and the external background plasma density. The semi-analytical solutions of the model appear in agreement with the complex numerical PIC simulations.

Besides of that, as an alternative to the traditionally considered electron cyclotron maser (ECM) mechanism of exoplanetary radio emission (RE), we consider the plasma maser mechanism. The latter, contrary to ECM operates in dense and weakly magnetized plasmas, where electron cyclotron frequency f_c is less than Langmuir frequency f_L . Similar mechanism is known to contribute the generation of RE in solar corona, as well as in magnetospheres of the Solar System planets. It is a two-step process. At first, the plasma waves are excited due to Cherenkov instability in a weakly anisotropic background plasma by a small admixture of hot electrons with a loss-cone type non-equilibrium distribution function. Then, the electromagnetic radiation at f_{RE} arises due to, e.g., plasma wave scattering on the background ions (Rayleigh scattering, $f_{RE} = f_L$), or nonlinear coupling of two plasma waves (Raman scattering, $f_{RE} = 2f_L$). In the first case, the maser effect at plasma frequency f_L takes place under certain conditions, leading to an exponential growth of the RE intensity with the growing energy of plasma waves. In the case of Raman scattering of two plasma waves, resulting in generation of the RE at doubled plasma frequency, the maser effect is absent, but the collisional dissipation of RE is significantly reduced at the same time. This improves the requirements regarding the brightness temperature of the RE source, to provide a detectable on Earth radiation flux. In both cases the frequency band of the exoplanetary RE is defined not by magnetic field, but by the structure of planetary plasmasphere and density distribution there.

References:

1. Alexeev, I.I., Parunakian, D., Dyadechkin, S., Belenkaya, E.S., Khodachenko, M.L., Kallio, E., Alho, M., Calculation of the Initial Magnetic Field for Mercury's Magnetosphere Hybrid Model, *Cosmic Research*, 2018, 56, No. 2, 108–114 (in Russian published in *Kosmicheskie Issledovaniya*, 2018, Vol. 56, No. 2, pp. 119–127) (DOI: 10.1134/S0010952518020028)
2. Arkhypov, O.V., Khodachenko, M.L., Empirically revealed properties of Rieger-type cycles of stellar activity, *Astron. & Astrophys.*, 2021, 651, A28 (DOI: <https://doi.org/10.1051/0004-6361/202140629>)
3. Arkhypov, O.V., Khodachenko, M.L., Hanslmeier, A., Revealing of peculiar exoplanetary shadows from transit light-curves, *Astron. & Astrophys.*, 2021, 646, A136 (DOI: <https://doi.org/10.1051/0004-6361/202039050>)
4. Arkhypov, O.V., Khodachenko, M.L., Hanslmeier, A., Variability of transit light curves of Kepler objects of interest, *Astron. & Astrophys.*, 2020, 638, A143 (<https://doi.org/10.1051/0004-6361/201937303>)
5. Arkhypov, O.V., Khodachenko, M.L., Hanslmeier, A., Dusty phenomena in the vicinity of giant exoplanets, *Astron. & Astrophys.*, 2019, 631, A152 (DOI: <https://doi.org/10.1051/0004-6361/201936521>)
6. Arkhypov, O. V., Khodachenko, M. L., Güdel, M., Lüftinger, T., & Johnstone, C. P., Timescales of starspot variability in slow rotators, *Astron. & Astrophys.*, 2018, 613, A31 (DOI: <https://doi.org/10.1051/0004-6361/201732032>, Open Access)
7. Arkhypov, O.V., Khodachenko, M.L., Lammer, H., Güdel, M., Lüftinger, T., Johnstone, C.P. Starspot variability as an X-ray radiation proxy. *Monthly Notices of the Royal Astronomical Society*, 2018, Vol. 476, No. 1, p.1224-1233 (DOI: 10.1093/mnras/sty301, Open Access).

8. Arkhypov, O. V., Khodachenko, M. L., Güdel, M., Lüftinger, T., & Johnstone, C. P., Timescales of stellar rotational variability and starspot diagnostics, *MNRAS*, 2018, 473, Issue 1, L84–L88 (DOI: <https://doi.org/10.1093/mnrasl/slx170>, Open Access)
9. Arkhypov, O.V., Khodachenko, M.L., Lammer, H., Güdel, M., Lüftinger, T., Johnstone, C.P., Deep Mixing in Stellar Variability: Improved Method, Statistics, and Applications *Astrophysical Journal*, 2016, 826, art.id. 35, (DOI:10.3847/0004-637X/826/1/35)
10. Arkhypov, O.V., Khodachenko, M.L., Lammer, H., Güdel, M., Lüftinger, T., Johnstone, C., Short-period Stellar Activity Cycles with Kepler Photometry, *Astrophysical Journal*, 2015, 807, Issue 1, art.id. 109 (DOI: 10.1088/0004-637X/807/1/109)
11. Arkhypov, O. V., Khodachenko, M.L., Güdel, M., Johnstone, C., Lüftinger, T., Lammer, H., Signs of deep mixing in starspot variability, *Astronomy & Astrophysics*, 2015, 576, art.id.A67 (DOI: 10.1051/0004-6361/201425307)
12. Bagashvili, S.R., Shergelashvili, B.M., Japaridze, D.R., Kukhianidze, V., Poedts, S., Zaqarashvili, T.V., Khodachenko, M.L., De Causmaecker, P., Evidence for Precursors of the Coronal Hole Jets in Solar Bright Points, *Astrophysical Journal Lett.*, 2018, 855, L21 (<https://doi.org/10.3847/2041-8213/aab08b>)
13. Bagashvili, S. R., Shergelashvili, B. M., Japaridze, D. R., Chargeishvili, B. B., Kosovichev, A. G., Kukhianidze, V., Ramishvili, G., Zaqarashvili, T. V., Poedts, S., Khodachenko, M. L., De Causmaecker, P., Statistical properties of coronal hole rotation rates: Are they linked to the solar interior? *Astronomy & Astrophysics*, 2017, 603, id.A134 (DOI: 10.1051/0004-6361/201630377)
14. Ballester, J.L., Alexeev, I.I., Collados, M., Downes, T., Pfaff, R.F., Gilbert, H., Khodachenko, M.L., Khomenko, E., Shaikhislamov, I.F., Soler, R., Vázquez-Semadeni, E., Zaqarashvili, T., Partially Ionized Plasmas in Astrophysics, *Space Sci. Rev.* 2018, 214:58 (<https://doi.org/10.1007/s11214-018-0485-6>)
15. Berezutsky, A.G., Shaikhislamov, I. F., Rumenskikh, M. S., Khodachenko, M.L., Lammer, H., Miroshnichenko, I.B., On the transit spectroscopy features of warm Neptunes in the TOI-421 system, revealed with their 3D aeronomy simulations, *MNRAS*, 2022, 515(1), 706–715 (DOI: 10.1093/mnras/stac1633)
16. Dididze, G., Shergelashvili, B. M., Melnik, V. N., Dorovskyy, V. V., Brazhenko, A. I., Poedts, S., Zaqarashvili, T. V., Khodachenko, M.L., Comparative analysis of solar radio bursts before and during CME propagation, *Astron. & Astrophys.*, 2019, 625, A63 (DOI: <https://doi.org/10.1051/0004-6361/201629489>)
17. Dumbadze, G., Shergelashvili, B.M., Poedts, S., Zaqarashvili, T.V., Khodachenko, M.L., De Causmaecker, P., Eigenspectra of solar active region long-period oscillations, *Astron. & Astrophys.*, 2021, 653, A39 (DOI: 10.1051/0004-6361/202038124)
18. Dumbadze, G., Shergelashvili, B. M., Kukhianidze, V., Ramishvili, G., Zaqarashvili, T. V., Khodachenko, M.L., Gurgenashvili, E., Poedts, S., De Causmaecker, P., Long-period oscillations of active region patterns: least-squares mapping on second-order curves *Astronomy & Astrophysics*, 2017, 597, art.id. A93 (DOI: 10.1051/0004-6361/201628213)
19. Dwivedi, N. K., Khodachenko, M.L., Shaikhislamov, I. F., Fossati, L., Lammer, H., Sasunov, Y.L., Berezutskiy, A. G., Miroshnichenko, I. B., Kislyakova, K. G., Johnstone, C. P., Güdel, M., Modelling atmospheric escape and Mg II near-ultraviolet absorption of the highly irradiated hot Jupiter WASP-12b, *MNRAS*, 2019, 487, 4208–4220 (DOI: 10.1093/mnras/stz1345)
20. Fossati, L., Guilluy, G., Shaikhislamov, I. F., Carleo, I., Borsa, F., Bonomo, A. S., Giacobbe, P., Rainer, M., Cecchi-Pestellini, C., Khodachenko, M.L., et al., The GAPS Programme at TNG. XXXII. The revealing non-detection of metastable He I in the atmosphere of the hot Jupiter WASP-80b, *Astron. & Astrophys.*, 2022, 658, A136 (DOI: 10.1051/0004-6361/202142336)
21. Khodachenko, M. L., Shaikhislamov, I. F., Fossati, L., Lammer, H., Rumenskikh, M.S., Berezutsky, A. G., Miroshnichenko, I. B., Efimov, M.A., Simulation of 10830 Å absorption with a 3D hydrodynamic model reveals the solar He abundance in upper atmosphere of WASP-107b, *MNRAS: Letters*, 2021, 503, Issue 1, L23–L27 (DOI: <https://doi.org/10.1093/mnrasl/slab015>)
22. Khodachenko M.L., Shaikhislamov, I.F., Lammer, H., Miroshnichenko, I.B., Rumenskikh, M.S., Berezutsky, A.G., Fossati, L., The impact of intrinsic magnetic field on the absorption signatures of elements probing the upper atmosphere of HD209458b, *MNRAS*, 2021, 507(3), 3626–3637 (DOI: 10.1093/mnras/stab2366)
23. Khodachenko, M.L., Shaikhislamov, I.F., Lammer, H., Berezutsky, A.G., Miroshnichenko, I.B., Rumenskikh, M.S., Kislyakova, K.G., Dwivedi, N.K., Global 3D hydrodynamic modeling of in-transit Ly α absorption of GJ436b, *ApJ*, 2019, 885:67 (DOI: <https://doi.org/10.3847/1538-4357/ab46a4>, Open Access)

24. Khodachenko, M.L., Shaikhislamov, I.F., Lammer, H., Kislyakova, K.G., Fossati, L., Johnstone, C.P., Arkhylov, O.V., Berezutsky, A.G., Miroshnichenko, I.B., Posukh, V.G., Ly α Absorption at Transits of HD 209458b: A Comparative Study of Various Mechanisms Under Different Conditions, *Astrophysical Journal*, 2017, 847:126 (<https://doi.org/10.3847/1538-4357/aa88ad>, Open Access)
25. Khodachenko, M.L., Shaykhislamov, I., Lammer, H., Prokopov, P.A., Atmosphere Expansion and Mass Loss of Close-Orbit Giant Exoplanets heated by Stellar XUV. II. Effects of Planetary Magnetic Field; Structuring of inner Magnetosphere, *Astrophysical Journal*, 2015, 813:50 (DOI: 10.1088/0004-637X/813/1/50)
26. Kislyakova, K. G., Johnstone, C. P., Scherf, M., Holmstroem, M., Alexeev, I. I., Lammer, H., Khodachenko, M. L., Guedel, M., Evolution of the Earth's polar outflow from mid-Archean to present, *JGR Space Phys.*, 2020, 125, e2020JA027837, (DOI: <https://doi.org/10.1029/2020JA027837>)
27. Owen, J.E., Shaikhislamov, I.F., Lammer, H., Fossati, L., Khodachenko, M.L., Hydrogen Dominated Atmospheres on Terrestrial Mass Planets: Evidence, Origin and Evolution, *Space Sci. Rev.*, 2020, 216, 129 (<https://doi.org/10.1007/s11214-020-00756-w>)
28. Parunakian, D., Dyadechkin, S., Alexeev, I.I., Belenkaya, E.S., Khodachenko, M.L., Kallio, E., Markku Alho, M., Simulation of Mercury's magnetosheath with a combined hybrid-paraboloid model, *J. Geophys. Res. Space Physics*, 2017, 122, 8310–8326, (doi:10.1002/2017JA024105)
29. Philishvili, E., Shergelashvili, B.M., Buitendag, S., Raes, J., Poedts, S., Khodachenko, M.L., Case study on the identification and classification of small-scale flow patterns in flaring active region, *Astron. & Astrophys.*, 2021, 645, id.A52 (DOI: 10.1051/0004-6361/202038895)
30. Philishvili, E., Shergelashvili, B. M., Zaqarashvili, T. V., Kukhianidze, V., Ramishvili, G., Khodachenko, M.L., Poedts, S., De Causmaecker, P., Quasi-oscillatory dynamics observed in ascending phase of the flare on March 6, 2012, *Astronomy & Astrophysics*, 2017, 600, art.id. A67 (DOI: 10.1051/0004-6361/201629495)
31. Rumenskikh, M. S., Shaikhislamov, I. F., Khodachenko, M.L., Lammer, H., Miroshnichenko, I.B., Berezutsky, A.G., Fossati, L., Global 3D simulation of the upper atmosphere of HD189733b and absorption in metastable HeI and Ly α lines, *ApJ*, 2022, 927(2), art.id.238 (DOI: 10.3847/1538-4357/ac441d)
32. Sasunov, Yu.L., Khodachenko, M.L., Kubyshkin, I.V., Dwivedi, N., Alexeev, I.I., Belenkaya, E.S., Malova, H.V., Kulminkaya, N., Transient particle acceleration by a dawn–dusk electric field in a current sheet, *Phys. of Plasmas*, 2021, 28, 042902 (DOI: <https://doi.org/10.1063/5.0037060>)
33. Sasunov, Yu.L., M.L. Khodachenko, I.I. Alexeev, E.S. Belenkaya, V.M. Gubchenko, N. Dwivedi, A. Hanslmeier: Self-consistent description of the tangential-discontinuity-type current sheet, using the particle trajectory method and angular variables, *Phys. Plasmas*, 2018, 25, 092110, (doi:10.1063/1.5044720)
34. Sasunov, Yu.L., Khodachenko, M.L., Alexeev, I.I., Belenkaya, E.S., Mingalev, O.V., Melnik, M.N., The influence of kinetic effect on the MHD scalings of a thin current sheet, *J. Geophys. Res. Space Physics*, 2017, 122, 493–500 (doi:10.1002/2016JA023162).
35. Sasunov, Yu. L., Semenov, V. S., Heyn, M. F., Erkaev, N. V., Kubyshkin, I. V., Slivka, K.Yu., Korovinskiy, D. B., Khodachenko, M. L., A statistical survey of reconnection exhausts in the solar wind based on the Riemannian decay of current sheets, *J. Geophys. Res. Space Physics*, 2015, 120, 8194-8209 (DOI:10.1002/2015JA021504)
36. Sasunov, Yu. L., Khodachenko M.L., Alexeev, I.I., Belenkaya, E.S., Gordeev, E.I., Kubyshkin I. V. , The energy-based scaling of a thin current sheet: case study, *Geophys. Res. Lett.*, 2015, 42, 9609-9616 (DOI: 10.1002/2015GL066189)
37. Sasunov, Yu. L., Khodachenko, M. L., Alexeev, I. I., Belenkaya, E. S., Semenov, V. S., Kubyshkin, I. V., Mingalev, O.V., Investigation of scaling properties of a thin current sheet by means of particle trajectories study, *J. Geophys. Res. Space Physics*, 2015, 120, 1633–1645, (DOI: 10.1002/2014JA020486)
38. Shaikhislamov, I.F., Khodachenko, M.L., Berezutskiy, A.G., The Atmospheric Wind of Hot Exoplanets and its Manifestations in Observations: from Energy Estimates to 3D MHD Models, *Astronomy Reports*, 2021, 65, 8-25 (DOI: 10.1134/S1063772921010054)
39. Shaikhislamov, I. F., Khodachenko, M. L., Lammer, H., Berezutsky, A. G., Miroshnichenko, I. B., & Rumenskikh, M. S., Global 3D hydrodynamic modeling of absorption in Ly α and He 10830 Å lines at transits of GJ3470b. *MNRAS*, 2020, (DOI: 10.1093/mnras/staa2367)
40. Shaikhislamov, I. F., Fossati, L., Khodachenko, M. L., Lammer, H., García Muñoz, A., Youngblood, A., Dwivedi, N. K., Rumenskikh, M. S., Three-dimensional hydrodynamic simulations of the upper atmosphere of π Men c: comparison with Ly α transit observations, *Astron. & Astrophys.*, 2020, 639, A109 (<https://doi.org/10.1051/0004-6361/202038363>).

41. Shaikhislamov, I.F., Khodachenko, M.L., Lammer, H., Berezutsky, A.G., Miroshnichenko, I.B., Rumenskikh, M.S., Three-dimensional modelling of absorption by various species for hot Jupiter HD 209458b, *MNRAS*, 2020, 491, 3435–3447 (DOI: <https://doi.org/10.1093/mnras/stz3211>)
42. Shaikhislamov, I.F., Khodachenko, M.L., Lammer, H., Berezutsky, A.G., Miroshnichenko, I.B., Rumenskikh, M.S., Three-dimensional modelling of absorption by various species for hot Jupiter HD 209458b, *MNRAS*, 2019, 491, 3435–3447 (DOI: <https://doi.org/10.1093/mnras/stz3211>, Open Access)
43. Shaikhislamov, I.F., M.L. Khodachenko, H. Lammer, A. G. Berezutsky, I. B. Miroshnichenko, M. S. Rumenskikh, 3D Aeronomy modelling of close-in exoplanets, *MNRAS*, 2018, 481, 5315–5323 (DOI: 10.1093/mnras/sty2652)
44. Shaikhislamov, I.F., Khodachenko, M.L., Lammer, H., Fossati, L., Dwivedi, N., Güdel, M., Kislyakova, K.G., Johnstone, C.P., Berezutsky, A.G., Miroshnichenko, I.B., Posukh, V.G., Erkaev, N.V., Ivanov, V.A., Modeling of absorption by heavy minor species for the hot Jupiter HD 209458b, *Astrophysical Journal*, 2018, 866:47 (<https://doi.org/10.3847/1538-4357/aadf39> Open access).
45. Shaikhislamov, I. F., Khodachenko, M.L., Lammer, H., Kislyakova, K.G., Fossati, L., Johnstone, C.P., Prokopov, P.A., Berezutsky, A.G., Zakharov, Yu.P., Posukh, V.G., Two rgimes of interaction of a Hot Jupiter’s escaping atmosphere with the stellar wind and generation of energized atomic hydrogen corona, *The Astrophysical Journal*, 2016, 832, art.id. 173 (DOI: <http://dx.doi.org/10.3847/0004-637X/832/2/173>)
46. Shergelashvili, B.M., Philishvili, E., Buitendag, S., Poedts, S., Khodachenko, M.L., Categorization model of moving small-scale intensity enhancements in solar active regions, *Astron. & Astrophys.*, 2022, 662, art.id.A30 (DOI: 10.1051/0004-6361/202142547)
47. Shergelashvili, B. M., Melnik, V.N., Dididze, G., Fichtner, H., Brenn, G., Poedts, S., Foysi, H., Khodachenko M.L., Zaqarashvili T.V., A new class of discontinuous solar wind solutions, *MNRAS*, 2020, 496, 1023–1034 (DOI: 10.1093/mnras/staa1396)
48. Shergelashvili, B. M., Melnik, V.N., Dididze, G., Fichtner, H., Brenn, G., Poedts, S., Foysi, H., Khodachenko M.L., Zaqarashvili T.V., A new class of discontinuous solar wind solutions, *MNRAS*, 2020, 496, 1023–1034 (DOI: 10.1093/mnras/staa1396)
49. Weber, C., Lammer, H., Shaikhislamov, I. F., Chadney, J. M., Khodachenko, M. L., Griebmeier, J.-M., Rucker, H. O., Vocks, C., Macher, W., Odert, P., Kislyakova, K. G., How expanded ionospheres of Hot Jupiters can prevent escape of radio emission generated by the cyclotron maser instability, *MNRAS*, 2017, 469, p.3505-3517 (DOI: 10.1093/mnras/stx1099).